Enhancement of Critical Heat Flux From High Power Microelectronic Heat Sources in a Flow Channel

Issam Mudawar
Associate Professor and Director of the Purdue University Boiling and Two-Phase Flow Laboratory.

Douglas E. Maddox
Graduate Research Assistant.

Boiling and Two-Phase Flow Laboratory,
School of Mechanical Engineering,
Purdue University,
West Lafayette, Ind. 47907

Several surface augmentation techniques were examined in an investigation of enhancement of critical heat flux (CHF) from a simulated electronic chip to a fluorocarbon (FC-72) liquid in a vertical channel. A parametric comparison of boiling performances is presented for a smooth surface and for surfaces with low-profile microgrooves, low-profile microstuds, and high-profile pin fins. Critical heat fluxes as high as 361 W/cm^2 were achieved using a combination of moderate flow velocity, high subcooling and surface enhancement. A semiempirical model constructed previously for CHF from a smooth discrete heat source to saturated or subcooled liquid flow, was found successful in correlating CHF data for the three enhanced surfaces.

Introduction

Increased power dissipation from electronic devices is expected to continue in the near future due to the continuing trends of increased circuit concentration in silicon chips and closer packaging of chips in multi-chip modules. The power dissipation densities at both the chip and module levels have already exceeded the capabilities of cutting-edge air cooling technologies, creating the need for direct immersion in liquid coolants.

Despite the existence of numerous direct immersion techniques for achieving high cooling rates in many of today's high-tech applications, these techniques cannot be employed in cooling computer systems due to a lack of compatibility of common liquid coolants with electronic hardware. Even using the proper coolant, many of these techniques would require extensive cooling hardware built around each chip, precluding their implementation with circuit boards packed with large arrays of closely spaced chips.

Unfortunately, the fluorocarbon liquids chemically and electrically compatible for direct immersion cooling of chips possess poor thermal transport properties relative to common fluids such as water. Hence, great emphasis has been placed in recent years on heat transfer enhancement techniques via extended surfaces and phase change (Simons, 1987).

The fluorocarbon liquid FC-72 (product of 3M Company) is the prime candidate for electronic cooling via pool or forced convection boiling since its boiling point is 56°C at atmospheric pressure. Hence, it is capable of maintaining chip surface temperature below the 85°C limit commonly accepted in the electronics industry as a safe standard against chip failure (Simons, 1983).

One major obstacle to the use of FC-72 for electronic cooling is its relatively low critical heat flux (CHF), the upper limit for boiling heat transfer desired for electronic cooling. For pool boiling, CHF for FC-72 at atmospheric pressure is estimated to be 20 W/cm^2 (Anderson and Mudawar, 1989). This value is far lower than the 100 W/cm^2 heat flux limit projected for high power chips of the mid-1990's (Bar-Cohen et al., 1986). Thus, further CHF enhancement is essential for meeting these electronic cooling challenges.

Phase change poses three technical problems which may potentially endanger the reliability of electronic devices. The first is the temperature excursion which accompanies the incipience of nucleate boiling of highly wetting fluids such as FC-72 (Marto and Lepere, 1982; Anderson and Mudawar, 1989). This excursion induces thermal cycling during power transients, which could cause eventual damage to the chip. The second problem is the growth of a bubble boundary layer over multichip modules, where some chips may be deprived of cooling due the vapor wake created by other chips. Hence, CHF enhancement techniques for a single chip may not be acceptable if these techniques promote excessive vapor buildup at the module level. A third problem which is commonly encountered in flow boiling systems is the excessive pressure drop associated with the streamwise increase in void fraction, requiring the use of large, powerful pumps for coolant circulation. Such pumps may not be tolerated in close proximity to advanced supercomputers.

Surface enhancement is a very popular tool for improving pool boiling performance. Marto and Lepere (1982) tested three commercial enhanced surfaces (Union Carbide High Flux, Hitachi Thermoexcel-E, and Wieland Gewa-T) in pool boiling. Compared to a plain copper surface, the commercial surfaces significantly shifted the boiling curves of FC-72 and R-113 toward lower superheats. Hwang and Moran (1981) reduced wall superheat in pool boiling of FC-72 by laser drilling a silicon chip surface with an array of cavities. They recorded a 50 percent increase in CHF with the same surface

Contributed by the Electrical and Electronics Packaging Division for publication in the JOURNAL OF ELECTRONIC PACKAGING. Manuscript received by the Electrical and Electronics Packaging Division February 22, 1990; revised manuscript received April 10, 1990.

compared to a smooth chip. Nakayama et al. (1984) achieved heat flux levels in excess of 100 W/cm^2 in FC-72 using a stud covered with miniature fins. Anderson and Mudawar (1989) performed a parametric investigation of four types of surface enhancement for pool boiling in FC-72: (1) surface roughness, (2) artificial cavities, (3) microgrooving, and (4) extended surfaces. Although all these techniques reduced wall superheat, significant CHF enhancement was observed only with machined microstructures and extended surfaces. Further details concerning heat transfer enhancement during pool boiling can be found in an article by Nakayama (1988).

Grimley et al. (1987) performed flow boiling experiments with FC-72 consisting of a liquid film falling over a vertical surface-augmented heat source. Surfaces with microgrooves machined in the direction of fluid flow produced the highest CHF compared to those with smooth or square microstud finish. With the aid of both still and video photography, they demonstrated that void fraction increases in the flow direction reaching its highest value at the trailing edge of the heater. Increasing heat flux ultimately resulted in separation of liquid from the heater, leaving a thin subfilm on the surface. CHF was triggered by an unsteady growth of a dry patch in the subfilm. Compared to the smooth surface, enhanced surfaces allowed surface tension forces to more effectively maintain contact between the liquid and the heated surface and inhibiting the lateral spread of dry patches.

A microstud surface similar in construction to that used by Grimley et al. was tested by Maddox and Mudawar (1988) with forced convection of FC-72 on simulated electronic chips. They demonstrated that the use of this low pressure drop microstud surface may be preferred for single-phase cooling of electronic chips over the use of heavily finned surfaces.

The present study aims at examining surface augmentation techniques in the enhancement of CHF from a simulated microelectronic chip in vertical channel flow. Critical heat flux correlations are presented for saturated and subcooled boiling of FC-72. The results are discussed in relevance to such important electronic cooling requirements as controlled buildup of void fraction and increased CHF.

Experimental Apparatus and Test Procedure

Flow Loop. Simulated chips with 12.7×12.7 mm^2 base area were flush mounted to one side of a vertical rectangular channel made from optical grade polycarbonate plastic. The chip was located 76 cm from the channel inlet, ensuring fully-developed flow at the test surface. As shown in Fig. 1, the flow was converged from the upstream reservoir via a streamlined nozzle followed by a honeycomb flow straightener. The flow was rejected into a downstream reservoir containing a coil-type water-cooled condenser. Liquid drained from the downstream reservoir into a magnetically-coupled centrifugal pump which routed the flow through a plate-type intercooler and a turbine flow meter and back into the upstream reservoir. Two electrical immersion heaters located in the reservoirs provided for initial fluid warmup and overcame heat loss from the loop during steady-state operation. An outlet at the upper section of the downstream reservoir was connected to an external pressurization system which facilitated independent temperature and pressure control during subcooled tests. Further details on the design and operation of the flow loop and pressurization system can be found in two previous articles by the authors (Mudawar and Maddox, 1988, 1989).

Heat Source Design. The high heat fluxes and severe temperature excursions associated with repeated CHF experiments demanded the use of a thermally optimized heat source electronically protected against physical burnout by a fast-acting power relay. The heat source consisted of nickel-chromium wire carefully inserted in a groove machined into the surface of a thermally conducting boron nitride ceramic plate as shown in Fig. 2. The wire was covered with another boron nitride plate, and the ceramic assembly inserted into an oxygen-free copper casing. Good thermal contact was maintained between the heat source and casing by machine screws which clamped a support cover against the assembly. The heater was mounted in a high temperature G-7 fiberglass flange which was mounted to one side of the flow channel. The back side of the heater was heavily insulated with perlite.

As shown in Fig. 3, each enhanced surface configuration was built upon an oxygen-free copper base plate with a surface area of 12.7×12.7 mm^2 and a thickness of 5.51 mm. Temperature measurements were obtained by thermocouples embedded at three longitudinal positions. As shown in Fig. 2, the base was flush-mounted in the flow channel, surrounded by a fiberglass adapter plate of identical thickness.

The chip base thermocouple were calibrated to within 0.1°C accuracy over wide ranges of temperature. During boiling experiments the thermocouple readings showed a maximum

Nomenclature

a = microstud height, m
A^+ = ratio of total wetted area to base area
A_b = chip base area, m^2
A_F = channel flow area, m^2
C = empirical constant in equation (1)
C_1 = empirical constant in equation (3)
c_{pf} = specific heat of liquid at constant pressure, J/(kg•K)
C_{sub} = subcooling constant
D = hydraulic diameter of flow channel $= 4A_F/P$, m
h_{fg} = latent heat of vaporization, J/kg
k_f = thermal conductivity of liquid, W/(m•K)
L = heater length in the flow direction, m
n = empirical constant in equation (1)
$\overline{Nu}_L$ = average Nusselt number based on heater length $= \dfrac{qL}{(T_w - T_m)k_f}$
P = wetted perimeter of flow area, m
Pr_f = liquid Prandtl number
q = heat flux, W/m^2
q_m = critical heat flux (CHF), W/m^2
Re_L = Reynolds number based on heater length $= \rho_f UL/\mu_f$
T_{CHF} = mean heater surface temperature at critical heat flux, °C
T_m = mean liquid temperature upstream of heater, °C
T_{sat} = saturation temperature, °C
T_w = mean temperature of heater surface, °C
ΔT_{sat} = wall superheat $= T_w - T_{sat}$, °C
ΔT_{sub} = liquid subcooling upstream of test heater $= T_{sat} - T_m$, °C
u = local liquid velocity parallel to heater surface, m/s
U = mean liquid velocity, m/s
y = distance normal to heated surface, m
δ_m = inlet thickness of liquid sublayer, m
μ_f = dynamic viscosity of liquid, kg/(m•s)
ρ_f = liquid density, kg/m^3
ρ_g = vapor density, kg/m^3
σ = surface tension, N/m

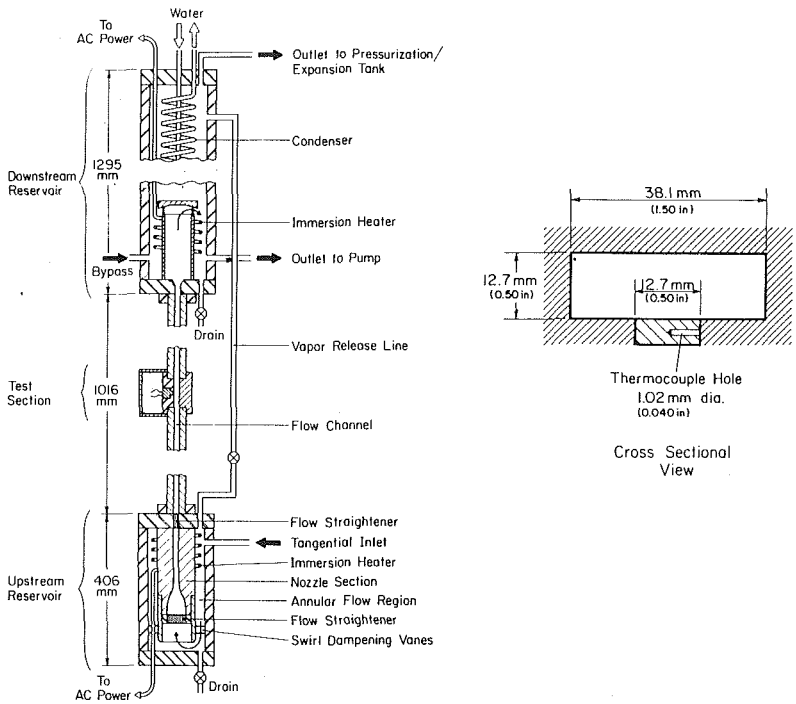

Fig. 1 Schematic diagram of the flow channel

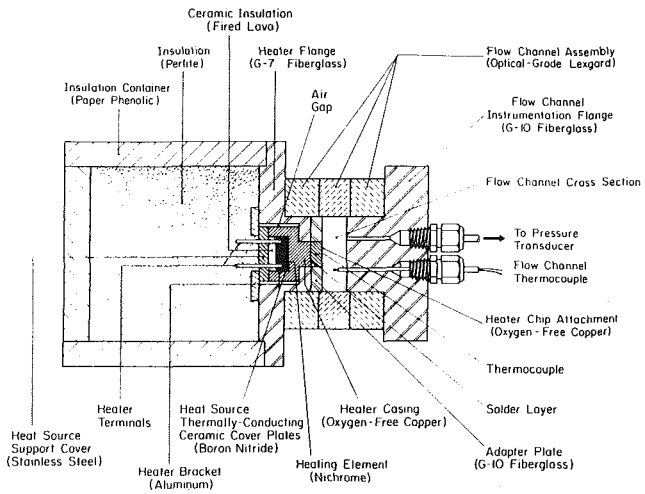

Fig. 2 Test heater construction

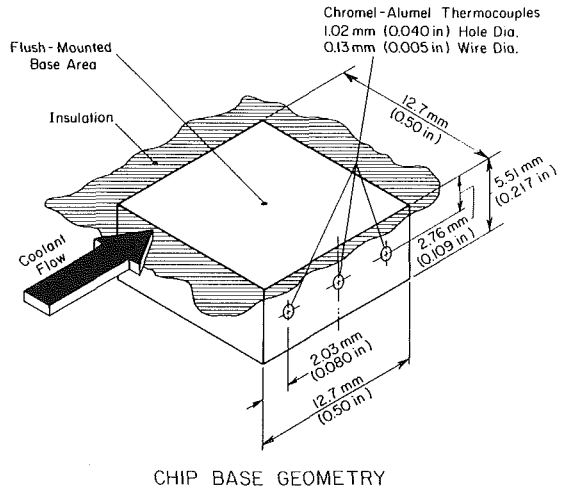

Fig. 3 Base chip geometry and dimensions

temperature difference of 2.2°C, with the middle thermocouple giving measurements within 0.5 percent of an average of the other two thermocouples.

The heater was powered by a 33 amp-80 volts Sorensen DC power supply equipped with a relay to switch off heater power upon detecting any overheating in the base. The heat flux was determined from the electrical power input corrected for heat loss. Several CHF experiments were repeated using the present heater and a calorimeter-type heater developed earlier by Maddox and Mudawar (1989). A nearly constant heat loss of 4 percent, determined from these calibration experiments, was corrected for in all the present data. Further details of the accuracies of temperature and heat flux measurements can be found in the two earlier articles by the authors (Maddox and Mudawar, 1988, 1989).

Enhanced Surface Geometries. The tests involved a smooth reference surface and several enhanced surfaces, all having a flush-mounted base area of 12.7×12.7 mm^2. As shown in Fig. 4, the enhanced surfaces included microstud surfaces with three different fin heights, a microgroove surface with a fin height equal to the tallest of the microstud surfaces, and a pin fin surface consisting of relatively large extended cylindrical fins. The high flow blockage geometry of this surface was tested to evaluate the level of enhancement this surface offers over microstructured surfaces. All surfaces were blasted with a high pressure stream of air, water and abrasive to ensure uniform surface microstructure prior to testing.

The low profile microgroove and microstud surfaces were chosen for their limited flow blockage, low pressure drop characteristics. Their short fins also limited bubble boundary layer thickening which is a primary concern in the cooling of chip arrays. Their fin spacing and pitch were based upon previous FC-72 boiling studies involving pool boiling (Nakayama et al., 1984; Anderson and Mudawar, 1989), and boiling in flowing liquid films (Mudawar et al., 1987). The maximum fin height of 1.02 mm was determined by a com-

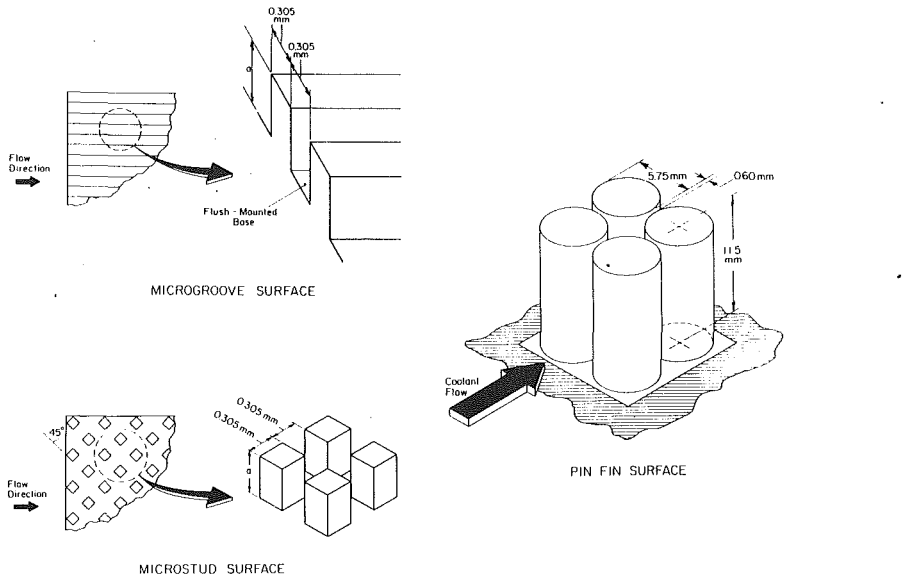

Fig. 4 Schematic diagrams of the enhanced surfaces

bination of machinability and fin strength constraints. The microgroove surface was fabricated by cutting grooves parallel to the flow direction, leaving fins with a height of 1.02 mm above the flush mounted base area. The microstuds were formed by two series of perpendicular cuts oriented 45 degrees with respect to the flow direction, leaving streamlined square studs. The heights of the studs for the three microstud surfaces were 0.25, 0.51, and 1.02 mm.

Since it is impossible to determine a single pin fin geometry that gives best performance for all flow conditions, the pin fin surface was numerically optimized based on a boiling curve determined experimentally for the smooth surface with a mid-range flow velocity of 2.25 m/s and near-saturated flow. Four fin arrangements were considered including a single large pin fin, and arrays of four, nine and sixteen equally spaced fins. Following the fin optimization method of Haley and Westwater (1965), all fins were assumed to experience local boiling conditions identical to those of a smooth surface at the same temperature. Experiments by Klein and Westwater (1971) using a nine pin array of boiling fins demonstrated that a bubble departure diameter was the optimal spacing for fin arrays. Thus, fin spacing in the present study was set conservatively equal to a bubble departure diameter of 0.61 mm measured experimentally for pool boiling ($U=0$) of FC-72. A maximum fin height of 11.8 mm was imposed by channel height and the desire to maintain boiling at the tip of the fin. For each of the four fin arrangements, a one-dimensional numerical computer program was used to calculate the base heat flux for the highest chip temperature guideline of 85°C. The surface with four fins, Fig. 4, was found to have the best performance, with a base heat flux slightly above that of the nine pin surface. Using an electric discharge machine (EDM), the four pin surface was machined from a single solid piece of copper to avoid the thermal contact resistance which would result from attaching pin fins to a separate base plate.

The ratios of total surface to base areas for all the enhanced surfaces of the present study are given in Table 1. Despite the large dimensions of the pins on the pin surface, it is obvious from Table 1 that its total surface area is only 46 percent greater than the low-profile microstud surface.

Test Procedure. Prior to each test, the immersion heaters of the two end reservoirs were energized to deaerate the liquid by vigorous boiling while liquid was being circulated in the loop. The mixture of fluorocarbon vapor and air was released into the external pressurization/expansion system, where air was rejected freely into the ambient while vapor was recondensed and captured in a condensate tank.

Table 1 Ratio of total heat transfer area to base area for the enhanced surfaces of the present study

Surface	Fin height (mm)	Ratio of heat transfer area to base area ($A_b = 1.613$ cm^2)
Smooth	0.00	1.00
Microgroove	1.02	4.34
Microstud	0.25	1.83
Microstud	0.51	2.67
Microstud	1.02	4.34
Pin fin	11.70	6.32

Following deaeration, liquid pressure and temperature were adjusted independently by controlling power supply to immersion heaters contained in the end reservoirs and pressurization/expansion tank, and by throttling water flow through the condenser coil and the flat plate intercooler.

Steady-state boiling curves were developed by increasing heater power in small increments separated by adequate waiting periods. Testing was terminated at CHF following an abrupt unsteady rise in heater temperature. Thermocouple readings and electrical power signals were monitored by a Keithley 500 data acquisition system and processed by a Compaq 286 microcomputer.

Results and Discussion

Experiments were performed with FC-72 at near-atmospheric pressure over a velocity range from 0.22 to 4.1 m/s and up to 48.9°C of subcooling. A series of experiments was performed in the single-phase region to correlate the convective heat transfer coefficient. In another series of tests, influence of flow velocity, subcooling and surface enhancement on the boiling curve was parametrically studied. A third series was aimed at obtaining only CHF data. The last set of experiments were initiated by setting power at a level within the fully developed boiling curve and increasing it in very small increments to locate the CHF point accurately.

Parametric tests were performed at a velocity of 2.25 m/s to

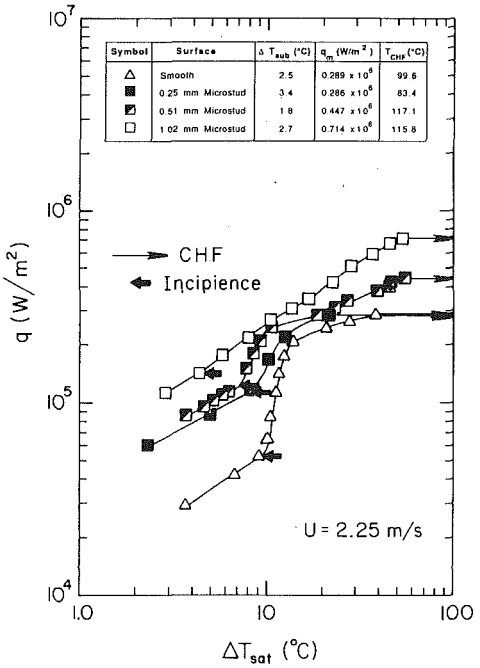

Fig. 5 Effect of microstud height on boiling performance

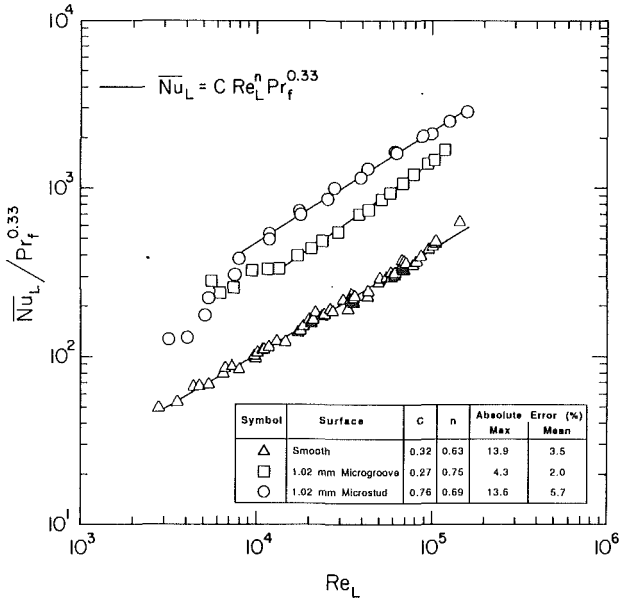

Fig. 6 Correlations for single-phase heat transfer from the smooth, microgroove, and microstud surfaces

assess the effects of microstud height on heat transfer performance in the single-phase and boiling regions. Compared to the smooth surface, the 1.02 mm microstud height increased the single-phase heat transfer coefficient and critical heat flux by factors of 4.8 and 2.5, respectively, with the intermediate fin heights giving lower enhancement factors as shown in Fig. 5. Videographic analysis of the boiling surface demonstrated that the grooves between microstuds did not behave as artificial nucleation sites because flow velocity significantly reduced bubble departure diameter compared to the width of these grooves. Small bubbles were observed on the microfin sides and base surface. As heat flux was increased further, boiling and bubble coalescence became more vigorous in these regions while smaller bubbles covered the fin tips. Thus, the increased surface area was a major contributing factor to the enhancement observed both in the single-phase and two-phase regions.

Single-phase data were correlated for the smooth, microgroove and tallest microstud over Reynolds numbers ranging from 2.8×10^3 to 1.48×10^5, 5.8×10^3 to 1.20×10^5, and 3.19×10^3 to 1.61×10^5, respectively. Both the average Nusselt number and the Reynolds number were based on heater length, and fluid properties were calculated at the mean fluid temperature upstream of the heater. As shown in Fig. 6, turbulent flow data for the three surfaces were fitted to the correlation

$$\overline{\mathrm{Nu}}_L = C\ \mathrm{Re}_L^n\ \mathrm{Pr}_f^{0.33} \qquad (1)$$

where the Prandtl number exponent was fixed at 0.33 following common turbulent channel flow correlations since the exponent could not be correlated within the limited Prandtl number range of the study. It should be noted that the empirical constants of equation (1) are unique to the low-profile enhanced surfaces used in the present study. A more universal correlation for the microgroove surface could include such additional dimensionless parameters as fin height-to-pitch ratio and fin height-to-width ratio. Figure 6 shows surface microstructures enhance single-phase heat transfer significantly compared to the smooth surface, with the microstud surface showing the best performance despite having a total wetted area, a fin height-to-pitch ratio and a fin height-to-width ratio identical to those of the microgroove surface. This suggests the microstud performance may also be dependent upon other parameters influencing liquid flow between and near the top surfaces of the microstuds. The enhancement of the microstud surface is complicated by a "serpentine" motion of liquid between adjacent rows of studs; nevertheless, its exceptional performance may be explained by the enhanced turbulent mixing and the development of multiple thermal entry regions at the top surfaces of individual studs. These effects are beyond the scope of the present CHF enhancement study.

Figure 7 shows a comparison of boiling performances of the three types of surface enhancement techniques along with smooth surface reference data. Although microstud surface performance is superior to the microgroove surface in the single-phase region, the microgroove surface displayed heat flux enhancement by a factor as high as 1.6 in the boiling region compared to the microstud surface, and a slight enhancement in CHF. The pin fin surface single-phase heat transfer coefficient was only 20 percent higher than that of the microstud surface despite its 46 percent greater surface area. In the boiling region, the heat transfer performance of the pin fin surface surpassed all other surfaces.

One disadvantage in operating with enhanced surfaces at saturated conditions is the large rate of vapor generation at high heat fluxes. This is especially a problem with the pin fin surface because it extends far into the channel. If an array of pin finned surfaces were to be mounted along a flow channel, the vapor generated from the upstream surfaces would quickly buildup over the downstream surfaces, causing the downstream surfaces to experience CHF at lower heat fluxes.

Flow visualization experiments showed that vapor buildup was greatly reduced by fluid subcooling. This reduction was actually greatest for the pin fin surface because the extended pins of this surface were more effective than microstructures in utilizing sensible heat exchange with subcooled flow. Figure 8 shows schematic diagrams of saturated and subcooled boiling on the pin fin surface. Contrary to the assumption of identical thermal performance for the four pins used in the numerical analysis of pin fin surface performance, partial boiling on the upstream pins created a vapor wake which totally engulfed the downstream pins. For saturated flow, the upstream portion of the pin tips did not experience boiling except for fluxes close to CHF. For subcooled flow, the bubbles were small to the point of not being detected by the naked eye

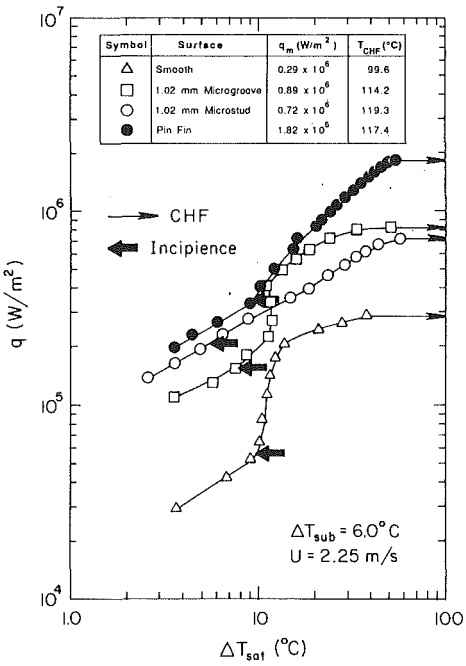

Fig. 7 Comparison of boiling performance of the smooth and enhance surfaces

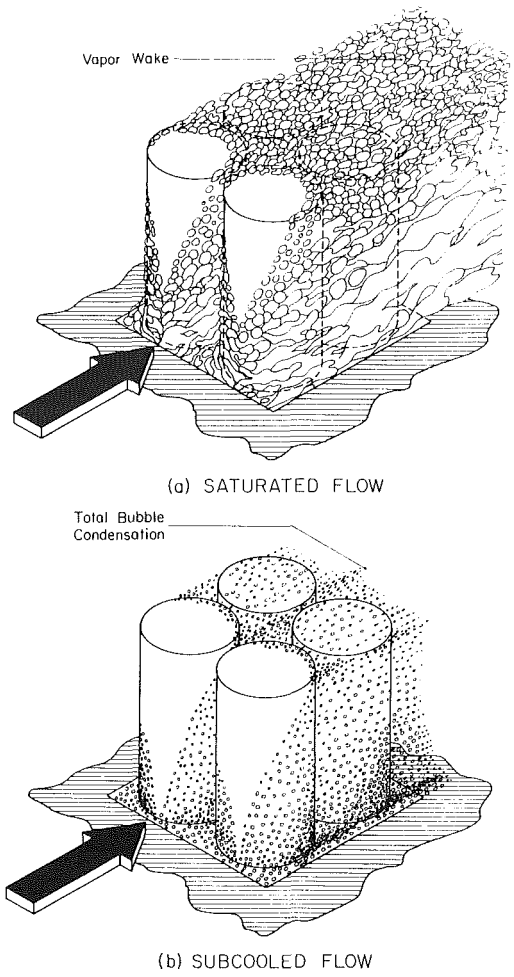

Fig. 8 Bubble boundary layer development on the pin fin surface for (a) saturated and (*b*) subcooled boiling

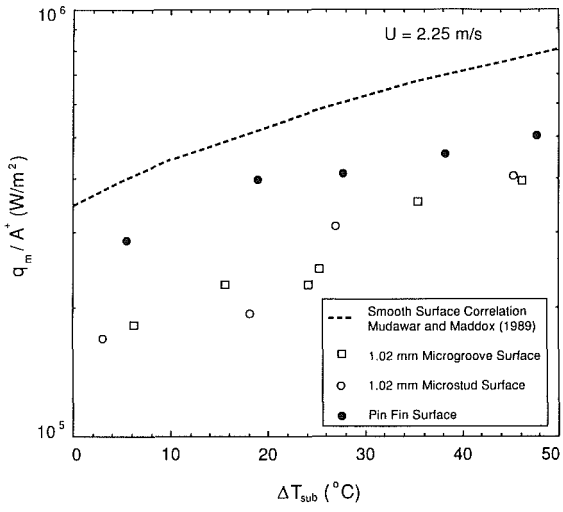

Fig. 9 Variation of CHF based upon total wetted area with subcooling for the smooth and enhanced surfaces

at high degrees of subcooling. The vapor wake disappeared by bubble condensation a very short downstream from the pins. This behavior demonstrates that subcooling may be necessary in the cooling of enhanced chip arrays to circumvent the problems of increased channel pressure drop and lower CHF values of downstream chips caused by increased void fraction.

Figure 9 shows the variation of critical heat flux based upon total wetted area with subcooling for the smooth and enhanced surfaces. The data reveal increasing surface area does not yield a proportionate increase in critical heat flux based on total area. The superior enhancement by the pin-fin surface over the microgroove and microstud surfaces can be explained by an ability of the protruded pins to more effectively utilize sensible heat exchange with the subcooled bulk liquid. Cross-flow over the pins also provides an effective means of supplying liquid to the boiling surface especially for the two front pins. In contrast, stream-wise vapor buildup near CHF makes the side and bottom walls of the microgrooves and microstuds ineffective at maintaining liquid contact despite the large areas of these surfaces. This phenomenon is evident from the large degradation in their CHF compared to the pin-fin surface, Fig. 9, especially at low ΔT_{sub}.

The highest heat transfer rates achieved in this study are shown in Fig. 10 for a fluid velocity of 4.1 m/s and high degrees of subcooling ranging from 44.9 to 48.9°C. The curves for the smooth and microstud surfaces include only boiling data because these experiments were performed solely for the determination of CHF. The CHF enhancement factors over the smooth surface were 2.08, 2.52, and 2.87, respectively, for the microstud, microgroove, and pin fin surfaces, with the pin fin surface reaching a CHF value of 361 W/cm^2. These enhanced surface CHF values are the highest reported for electronic cooling using a dielectric fluid in a practical configuration especially suited for cooling large arrays of chips.

The present results demonstrate that enhanced surfaces offer significant improvement in chip heat transfer performance. However, the low-profile microstructured surfaces may be preferred to the pin surface due to their limited flow blockage. For single-phase cooling the microstud surface is an ideal choice for enhancement, trailing pin fin surface performance only by a 20 percent reduction in heat transfer coefficient. For two-phase cooling, microstructured surfaces may provide adequate enhancement except for very high power chips which may necessitate the use of heavily finned attachments.

CHF Correlations. Many recent studies seem to link CHF to the dryout of a thin liquid sublayer beneath large vapor

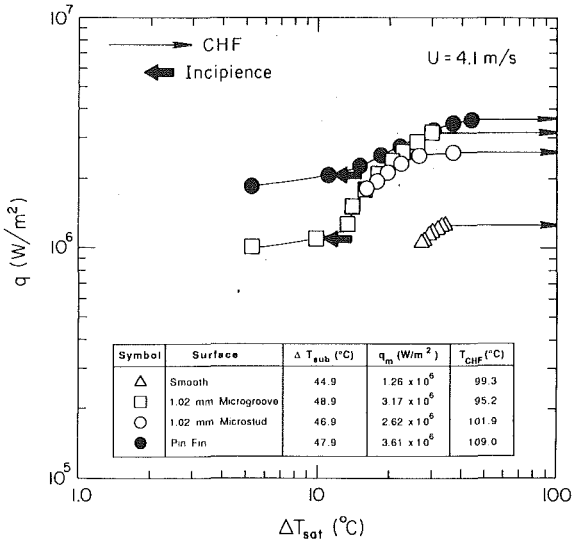

Fig. 10 Upper performance boiling curves for the smooth and enhanced surfaces

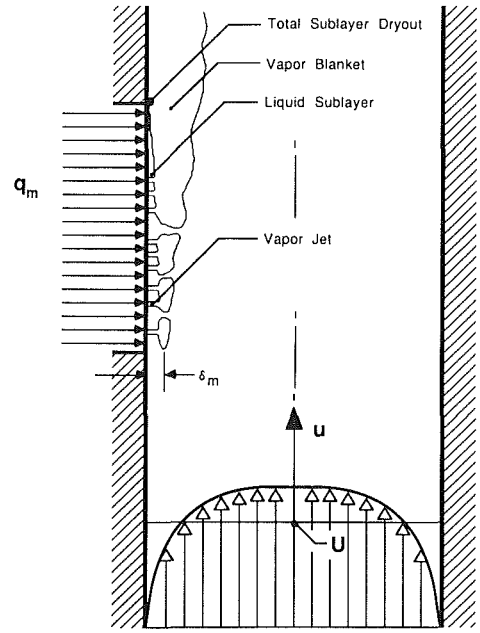

Fig. 11 Schematic representation of CHF from a smooth discrete heat source in a flow channel

bubbles accumulated near the surface during vigorous boiling. Gaertner (1965) demonstrated that, during fully developed pool boiling, vapor is released in jets normal to the heated surface. As heat flux approached CHF, the vapor jets broke down due a Helmholtz instability of the vapor-liquid interface, merging jets together and resulting in the formation of a vapor blanket near the surface. Gaertner presented photographic evidence of the existence of a liquid sublayer between the vapor jets which is trapped at the surface following jet breakdown.

Haramura and Katto (1983) developed CHF relations for saturated flow boiling systems by assuming that burnout occurs when the rate of evaporation of sublayer liquid exceeds that of liquid supply from the bulk region into the sublayer.

Mudawar et al. (1987, 1989) extended the applicability of the Haramura and Katto model to subcooled flow. They assumed a liquid sublayer thickness, δ_m, proportional to the wavelength of the Helmholtz instability of the interface between the vapor outflow jets and the liquid inflow towards the wall between the vapor jets.

Table 2 CHF correlation constants for the smooth and enhanced surfaces of the present study

Surface	C_1	C_{sub}	Mean absolute deviation
Smooth	0.161	0.021	7.1%
Microgroove	0.252	0.049	5.3%
1.02 mm microstud	0.244	0.066	7.0%
Pin fin	0.732	0.017	3.0%

For a smooth discrete heat source of length L flush-mounted in one wall of a flow channel, they hypothesized that CHF occurs when liquid entering the sublayer upstream just begins to dry out at the downstream edge of the heater as shown in Fig. 11. This implies

$$q_m L \geq \rho_f (c_{pf} \Delta T_{sub} + h_{fg}) \int_0^{\delta_m} u \, dy \tag{2}$$

where the velocity u was determined from a 1/7 power-low profile typical of a turbulent boundary layer. Their analysis resulted in the following subcooled CHF criterion:

$$\frac{q_m/(\rho_g h_{fg})}{U} = C_1 \left(\frac{\rho_f}{\rho_g}\right)^{15/23} \left[\frac{\sigma}{\rho_f U^2 L}\right]^{8/23} \left(\frac{L}{D}\right)^{1/23} \times \left[1 + \frac{c_{pf}\Delta T_{sub}}{h_{fg}}\right]^{7/23} \left[1 + C_{sub} \frac{\rho_f c_{pf} \Delta T_{sub}}{\rho_g h_{fg}}\right]^{16/23} \tag{3}$$

where D is the hydraulic diameter of the flow channel. The empirical constants of the CHF model ($C_1 = 0.161$ and $C_{sub} = 0.021$) were correlated by Mudawar and Maddox (1989) using atmospheric pressure FC-72 data obtained for the smooth surface of the present study.

Since surface enhancement has a strong influence on liquid sublayer formation and dryout, flow visualization was employed to monitor the development of the vapor blanket just prior to CHF for each of the enhanced surfaces. The microgroove and microstud surfaces were encased with thick blankets which protruded beyond the tips of the microstructures. As in the case of the smooth surface, CHF was triggered by dryout of liquid beneath the blanket. The blanket was much larger and more pronounced with the pin fin surface, and the pattern of liquid dryout was more complicated and less visible compared to the other surfaces.

The effects of velocity and subcooling on CHF for the enhanced surfaces were correlated empirically using equation (3). The correlation constants C_1 and C_{sub} for these surfaces are given in Table 2 along with the mean absolute deviation of the data from the corresponding correlations. These correlation are plotted in Fig. 12 for near-saturated conditions. Figure 13 shows the enhancement effect of subcooling on CHF for a mid-range flow velocity of 2.25 m/s. The accuracy of equation (3) in correlating the enhanced surface data is a strong evidence of the similarity of CHF mechanisms for smooth and enhanced surfaces.

Summary

The present study involved an examination of several surface augmentation techniques in an investigation of enhancement of CHF from a simulated microelectronic chip. Key results from the study are as follows:

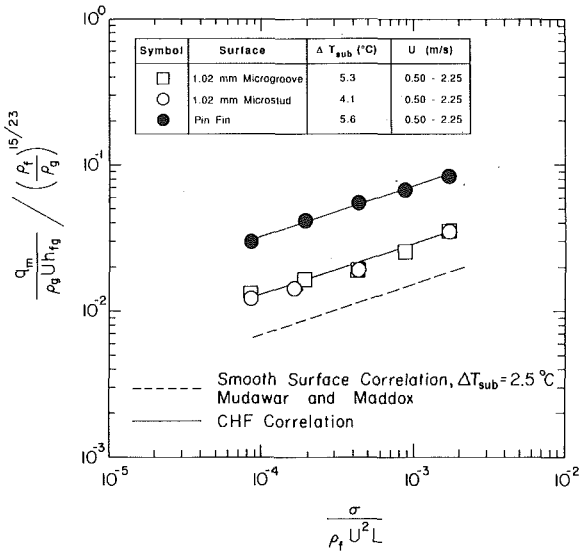

Fig. 12 Dimensionless CHF correlations for near-saturated conditions

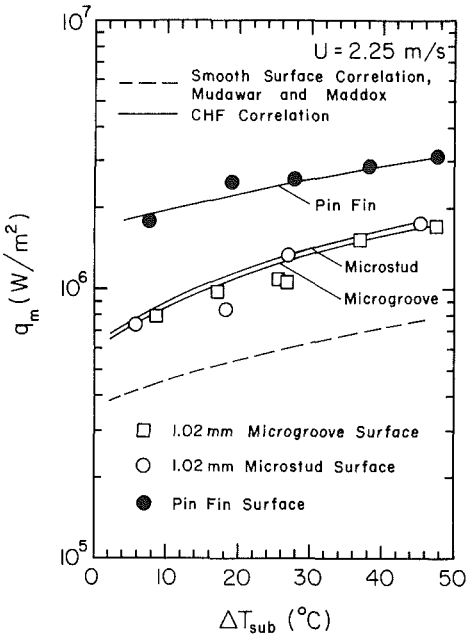

Fig. 13 Variation of CHF with subcooling

1. Although the relatively large pin fin surface showed the best cooling performance, low-profile microstructured surfaces may be preferred for electronic cooling due to their limited flow blockage. The microstud surface is ideal for single-phase cooling, trailing pin fin surface performance only by a 20 percent reduction in heat transfer coefficient. Microstructured surfaces are also suited for two-phase heat transfer enhancement except for very high power chips which may necessitate the use of heavily finned attachments.

2 Subcooling greatly reduces vapor buildup on enhanced surfaces. This reduction was greatest for the pin fin surface because the extended pins of this surface were more effective than microstructures in utilizing sensible heat exchange with the subcooled flow. Subcooling may be necessary in the cooling of enhanced chip arrays to circumvent the problems of increased channel pressure drop and lower CHF values of downstream chips caused by increased void fraction.

3 A combination of moderate coolant velocity and high degree of subcooling produced CHF values of 262, 317, and 361 W/cm^2 for the microstud, microgroove and pin fin surfaces, respectively. These values are the highest reported for electronic cooling using a dielectric fluid in a practical configuration especially suited for cooling large arrays of chips.

4 A sublayer dryout model previously developed for subcooled boiling CHF from a smooth surface in a flow channel was successful in correlating CHF data for the three types of surfaces considered in the present study. Thus, it may be hypothesized that the CHF mechanism of sublayer dryout is similar for all these surfaces.

Acknowledgment

Support for this research by the IBM Corporation is gratefully acknowledged. The authors also appreciate receiving FC-72 fluid samples from the Industrial Chemical Products Division of 3M.

References

Anderson, T. M., and Mudawar, I., 1989, "Microelectronic Cooling by Enhanced Pool Boiling of a Dielectric Fluorocarbon Liquid," ASME *Journal of Heat Transfer*, Vol. 111, pp. 752–759.

Bar-Cohen, A., Mudawar, I., and Whalen, B., 1986, "Future Challenges for Electronic Cooling," *Research Needs in Electronic Cooling*, F. P. Incropera, ed., published by the National Science Foundation and Purdue University, West Lafayette, IN, pp. 70–77.

Gaertner, R. F., 1965, "Photographic Study of Nucleate Pool Boiling on a Horizontal Surface," ASME *Journal of Heat Transfer*, Vol. 87, pp. 17–29.

Grimley, T. A., Mudawar, I. A., and Incropera, F. P., 1988, "CHF Enhancement in Flowing Fluorocarbon Liquid Films Using Structured Surfaces and Flow Deflectors," *Int. J. Heat Mass Transfer*, Vol. 31, pp. 55–65.

Haley, K. W., and Westwater, J. W., 1966, "Boiling Heat Transfer from Single Fins," *Proc. 3rd Int. Heat Transfer Conf.*, Vol. 3, pp. 245–258.

Haramura, Y., and Katto, Y., 1983, "A New Hydrodynamic Model of Critical Heat Flux Applicable Widely to both Pool and Forced Convection Boiling on Submerged Bodies in Saturated Liquids," *Int. J. Heat Mass Transfer*, Vol. 26, pp. 389–399.

Hwang, U. P., and Moran, K. P., 1981, "Boiling Heat Transfer of Silicon Integrated Circuits Chip Mounted on a Substrate," *Heat Transfer in Electronic Equipment*, HTD-Vol. 20, M. D. Kelleher and M. M. Yovanovich, eds., ASME, pp. 53–59.

Klein, G. J., and Westwater, J. W., 1971, "Heat Transfer from Multiple Splines to Boiling Liquids," *AIChE J.*, Vol. 17, pp. 1050–1056.

Maddox, D. E., and Mudawar, I., 1989, "Single and Two-Phase Convective Heat Transfer from Smooth and Enhanced Microelectronic Heat Sources in a Rectangular Channel," ASME *Journal of Heat Transfer*, Vol. 111, pp. 1045–1052.

Marto, P. J., and Lepere, V. J., 1982, "Pool Boiling Heat Transfer from Enhanced Surfaces to Dielectric Fluids," ASME *Journal of Heat Transfer*, Vol. 104, pp. 292–299.

Mudawar, I. A., Incropera, T. A., and Incropera, F. P., 1987, "Boiling Heat Transfer and Critical Heat Flux in Liquid Films Falling on Vertically-Mounted Heat Sources," *Int. J. Heat Mass Transfer*, Vol. 30, pp. 2083–2095.

Mudawar, I., and Maddox, D. E., 1989, "Critical Heat Flux in Subcooled Flow Boiling of Fluorocarbon Liquid on a Simulated Electronic Chip in a Vertical Rectangular Channel," *Int. J. Heat Mass Transfer*, Vol. 32, pp. 379–394.

Nakayama, W., Nakajima, T., and Hirasawa, S., 1984, "Heat Sink Studs Having Enhanced Boiling for Cooling of Microelectronic Components," ASME paper No. 84-WA/HT-89.

Nakayama, W., 1988, "Thermal Management of Electronic Equipment: A Review of Technology and Research Topics" *Advances in Thermal Modeling of Electronic Components and Systems*, A. Bar-Cohen and A. D. Krause, eds., Hemisphere Publishing Co., N.Y.

Simons, R. E., 1983, "Thermal Management of Electronic Packages," *Solid State Technology*, pp. 131–137.

Simons, R. E., 1987, "Direct Liquid Immersion Cooling: Past, Present, and Future," IBM Technical Report No. TR 00.3465, Poughkeepsie, NY.